Agricultural Water Management 264 (2022) 107502

Contents lists available at ScienceDirect

Agricultural Water Management

journal homepage: www.elsevier.com/locate/agwat

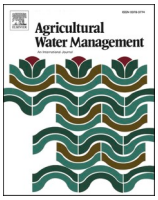

Nonlinear model predictive control of salinity and water level in polder networks: Case study of Lissertocht catchment

Boran Ekin Aydin [a,b,*], Gualbert H.P. Oude Essink [c,d], Joost R. Delsman [c], Nick van de Giesen [a], Edo Abraham [a]

[a] Department of Water Management, Delft University of Technology, Delft 2628CN, The Netherlands
[b] Operational Water Management, Nelen & Schuurmans, Utrecht 3511AE, The Netherlands
[c] Department of Subsurface and Groundwater, Deltares, Utrecht 3508AI, The Netherlands
[d] Department of Physical Geography, Utrecht University, 3584CS Utrecht, The Netherlands

ARTICLE INFO

Handling Editor - Dr Z Xiying

Keywords:
Groundwater exfiltration
Irrigation
Nonlinear Model Predictive Control (NMPC)
Nonlinear optimization
Polder
Salinity
Water quality control

ABSTRACT

A significant increase in surface water salinization in low-lying deltas is expected globally due to saline groundwater exfiltration driven by rising sea levels and decreasing freshwater availability. Sustaining fresh water-dependent agriculture in such areas will entail an increased demand for fresh water flushing. Unfortunately, the flushing of surface water is not operationally optimised and results in excessive use of scarce freshwater. To meet the increased demand for flushing, while minimizing the need for diverted freshwater, new operational designs are required. This paper presents a novel network model based approach that uses De Saint Venant (SV) and Advection Dispersion (AD) equations to optimize multiple objectives on water level and salinity control using a Nonlinear Model Predictive Control (NMPC). The resulting NMPC problem is solved with a receding horizon implementation, where the nonlinear program (NLP) at each iteration is solved using state-of-the-art large scale interior point solver (IPOPT). We evaluate the performance of the proposed approach and compare it to the traditional fixed flushing for a representative Dutch polder. Firstly, the approach is shown to be capable of controlling the water level and salinity level in the polder. Secondly, the results highlight that the network of canals, which were originally made for drainage, could not be made sufficiently fresh with current intake capacity. A simple design approach was used to identify appropriate new capacities for two of the gates that allow optimal flushing to guarantee the required water level and salinity constraints.

1. Introduction

Polders are low-lying, artificially drained embanked lands surrounded by storage canals (Fig. 1). Although The Netherlands is associated with polders (totaling around 4000 nationwide), polders are found in coastal areas across the world Delsman (2015)). Dominant land use in polders is mostly agriculture. Elevations of polders are generally below the surrounding area resulting in a necessity for continuous drainage of excess water using a dense network of water canals or ditches in the polder Delsman (2015)). Water levels in polder networks are kept within a predefined narrow margin using both intake structures and pumping stations. Accumulated storm water in the polder is transported to the pumping station and is pumped out of the polder onto the surrounding water storage canals (the so-called boezems). Water storage canals are used for providing extra freshwater during dry periods to replenish precipitation deficits, and for creating storage space for the surplus water from polders during wet periods (Schoubroeck and Kool, 2010; Agricultural activities as well as the freshwater ecosystem in the polders are threatened by surface water salinization due to saline groundwater exfiltration De Louw et al., 2011; Raats, 2015). Land subsidence, climate change and sea level rise increase the salinization of polders by enhancing the salt water intrusion rate Oude Essink et al. (2010)).

To maintain an acceptable salinity level, freshwater diverted from rivers is used to flush the polder and keep the surface water salinity levels below a certain threshold while not violating the water level constraints of the system. Current practice of flushing control generally relies on constant flushing where the inlet culverts are kept open while the resulting excess water is pumped out from the other side of the polder. Typically, this lasts from the beginning until the end of the crop

* Corresponding author at: Department of Water Management, Delft University of Technology, Delft 2628CN, The Netherlands.
E-mail addresses: boranekin@gmail.com, b.e.aydin@tudelft.nl (B.E. Aydin).

https://doi.org/10.1016/j.agwat.2022.107502
Received 22 April 2021; Received in revised form 17 January 2022; Accepted 20 January 2022
Available online 4 February 2022

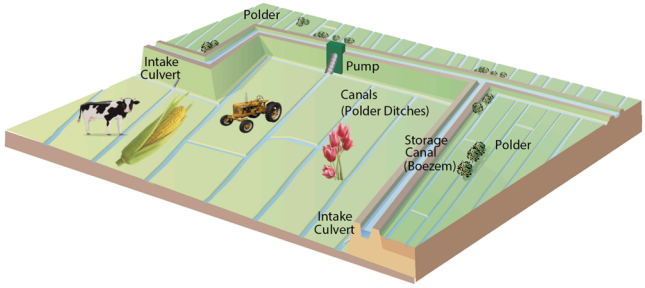

Fig. 1. Schematic overview of a polder system.
(Adapted from Delsman, 2015).

growing season resulting in excess use of freshwater and unnecessary pumping (Delsman, 2015); de Louw et al., 2011; Alfonso et al., 2010). In the Netherlands, 15% of total freshwater supply is currently used for surface water flushing Klijn et al. (2012)) and efficient surface water flushing is listed as a necessity to decrease surface water demand (Delta Programme Commissioner, 2019). Efficient water management in polders should aim to regulate water levels, salinity levels and fresh water usage by manipulating the intake and pump flows. Therefore, the operational control objectives for this case study implemented in this manuscript is selected as: .

- Water level needs to stay between predetermined thresholds (always) for safety, demand satisfaction and to maintain groundwater levels in operational limits for the drainage system,
- Salinity level needs to be below a certain threshold (when necessary) for agricultural and ecological usage, and
- Feshwater use and pumping cost should be minimized.

The relation between these sub-objectives may be conflicting: additional freshwater from the intakes is necessary to satisfy the salinity level objective, which will result in increased usage of freshwater and pump flows. This may result in violations of water levels, resulting in a complex multi-objective control problem. An advanced control algorithm for polder flushing to control salinity level and water quantity will increase the efficiency of the system.

Model predictive control (MPC) is a popular technique and has been used in the control of water systems including drinking water networks (Sampathirao et al., 2017), irrigation systems (Shang et al., 2019); Delgoda et al., 2016; Aydin et al., 2016; Romero et al., 2012; Hassani et al., 2019), flood control (Tian et al., 2015) and polders (Aydin et al., 2019b; Xu et al., 2013). If the processes that are controlled are regulated around a fixed operating point, the process models can be linearized. This allows the application of linear MPC (Kayacan et al, 2014) as applied in (Aydin et al., 2019b) for optimal salinity and water level control of water courses. However, in operation of a polder network, different salinity thresholds can be considered according to the farmer needs depending on the type and salt tolerance of the crop cultivated. A crop with low salt tolerance will require better water quality (low salinity concentration in the polder) than a crop with high salinity tolerance. To achieve sustainable irrigation water management, the possible variation in time and space of salinity threshold should be considered in the design of the controller. Moreover, spatial and temporal variation of saline groundwater disturbances make local linearization inefficient in terms of future system behaviour predictions. Here we consider a NMPC strategy that is based on the receding horizon principle. It can optimize the predicted future system behaviour by solving a nonlinear program (NLP) on-line at each control time step Tavernini et al. (2018)) and has been used for water systems in (Nederkoorn et al., 2012; Wang et al., 2017). The main advantage of NMPC is the ability to explicitly implement the constraints on inputs, outputs and states in the optimization problem (Kayacan et al., 2014).

For water quality (salinity) and quantity control, model based approaches have also been used in literature, where an MPC strategy to control the average salinity concentration in a ditch using a reservoir model have been considered in Xu et al. (2013, 2010). This study was followed by applying a model reduction technique for an internal model to control downstream salinity concentration in open channels. In a recent study, we achieved point salinity control in a single pool by explicitly considering freshwater conservation, using linearized Saint Venant (SV) and advection dispersion (AD) equations as the internal model of the MPC scheme (Aydin et al., 2019b). We used real saline groundwater exfiltration data for the first time to test the developed MPC scheme. Although the results were promising, the formulations of the previous studies were limited to either control of channels connected in series or controlling the (average) salinity at one location only. Our previous study (Aydin et al., 2019b) was the first attempt to minimize the freshwater usage but it was limited to the control of single channel. In a real polder network, multiple channels with different salinity concentrations are connected with or without hydraulic structures in between them. Mixing at the connection nodes is very important since the inflow concentration of downstream channels depend on the concentration of the upstream channels. Therefore, mixing at the connection nodes and the spatially varying salinity concentrations in a polder should be considered in optimization for polder flushing.

Motivated by the above-mentioned arguments, we propose in this study a novel NMPC framework for efficient flushing control in low-lying polders. To the best knowledge of the authors, this is the first case where a (real-world) polder network is controlled with a NMPC framework to achieve the dynamic control that respects water quality (salinty) needs in time and space. We first formulate the NMPC problem based on SV and AD equations to model the dynamics of the water and salt transport in the polder for flushing. Subsequently, parameters and constraints of the model are defined. In this work, we follow the direct collocation approach of 'first discretize and then optimize' for dynamical systems Betts (2010), where the optimal control problem is discretized and parametrized resulting in a nonlinear programming (NLP) problem. At each control time step, the NLP problem is solved over the prediction horizon and only the control action for the first time step is implemented with a receding horizon principle, where the prediction and optimal control calculations are repeated as the prediction horizon slides along. In this study, we use a state-of-the-art open-source optimization software IPOPT (Wächter and Biegler, 2006) to solve the resulting NLPs. Simulation examples of flushing control of a representative Dutch polder, the Lissertocht catchment, are presented to illustrate the closed-loop performance of the developed NMPC scheme as a case study. Finally, we investigate the results and suggest an improvement to the performance of the controller by upgrading the fresh water intake capacities of the polder.

2. System model

Transport of water and dissolved matter have to be considered to model the flushing of a polder (Hof and Schuurmans, 2000). For a single channel, these dynamics are described by Saint Venant (SV) Eq. (1) and one-dimensional Advection Dispersion (AD) Eq. (2) equations, respectively:

$$\begin{aligned} &\frac{\partial A}{\partial t}+\frac{\partial Q}{\partial z}=q_l, \\ &\frac{\partial Q}{\partial t}+\frac{\partial (Qu)}{\partial z}+gA\frac{\partial \zeta}{\partial z}+g\frac{Q|Q|}{C_z RA}=0, \end{aligned} \tag{1}$$

$$\frac{\partial AC}{\partial t}+\frac{\partial QC}{\partial z}=\frac{\partial}{\partial z}(KA\frac{\partial C}{\partial z})+q_l C_l, \tag{2}$$

where A is the cross sectional area [m^2], Q is the flow [m^3/s], q_l is the lateral inflow per unit length [$m^3/s/m$], u is the mean velocity (Q/A) [m/s], ζ is the water depth above the reference plane [m], $C_z = 40$ is the

Chezy coefficient [$m^{1/2}/s$], R is the hydraulic radius (A/P_f) [m], P_f is the wetted perimeter [m] and g is the gravity acceleration [9.8 m/s^2], K is the longitudinal dispersion coefficient [m^2s], C is the salt concentration [kg/m^3], C_l is the lateral flow concentration [kg/m^3], t is time [s] and z is horizontal dimension [m] (the choice of z instead of x as the horizontal dimension is to avoid confusion in the remainder of the paper where x is a vector representing the states of a system). The longitudinal dispersion coefficient (K) is given byFischer et al. (2013) as:

$$K = 0.011\frac{B^2u^2}{du_s}, \tag{3}$$

where B is the mean width [m], d is the mean water depth [m], $u_s = (gRS_b)^{1/2}$is the shear velocity [m/s] and S_b is the bottom slope of the canal [-]. In this paper, Eqs. (1) and (2) are discretized as in Xu et al. (2013), using a staggered grid and applied for both simulating the polder system and as the dynamic model of the NMPC design which is implemented in MATLAB®. Discretized SV and AD equations are organized in a compact matrix form such that all the terms with the next time step $k+1$ are kept at the left side while all the terms with the current time step k are left at the right side of the equation. In Eq. (4), system dynamics of a single channel with $n = 3$ discretization points is provided to illustrate the structure of the system dynamics matrix used at the rest of the paper.

$$\underbrace{\begin{bmatrix} sv_{11} & sv_{12} & & & 0 & \\ sv_{21} & sv_{22} & sv_{23} & & & \\ & sv_{32} & sv_{33} & & & \\ & & & ad_{11} & ad_{12} & \\ & 0 & & ad_{21} & ad_{22} & ad_{23} \\ & & & & ad_{32} & ad_{33} \end{bmatrix}^{k+1}}_{E_j^{k+1}\in\mathbb{R}^{(2n)\times(2n)}} \underbrace{\begin{bmatrix} h_1 \\ h_2 \\ h_3 \\ c_1 \\ c_2 \\ c_3 \end{bmatrix}^{k+1}}_{x_j^{k+1}\in\mathbb{R}^{(2n)}} =$$

$$\underbrace{\begin{bmatrix} 1 & & & & 0 & \\ & 1 & & & & \\ & & 1 & & & \\ & & & ad_{11} & & \\ & 0 & & & ad_{22} & \\ & & & & & ad_{33} \end{bmatrix}^{k}}_{A_j^k\in\mathbb{R}^{(2n)\times(2n)}} \underbrace{\begin{bmatrix} h_1 \\ h_2 \\ h_3 \\ c_1 \\ c_2 \\ c_3 \end{bmatrix}^{k}}_{x_j^k\in\mathbb{R}^{(2n)}} + \underbrace{\begin{bmatrix} sv_f & 0 \\ 0 & 0 \\ 0 & sv_o \\ ad_f & 0 \\ 0 & 0 \\ 0 & ad_o \end{bmatrix}^{k}}_{B_{u_j}^k\in\mathbb{R}^{(2n)\times(2)}} \underbrace{\begin{bmatrix} Q_{in} \\ Q_{out} \end{bmatrix}^{k}}_{u_j^k\in\mathbb{R}^{(2)}} + \underbrace{d^k}_{d_j^k\in\mathbb{R}^{(2n)}} \tag{4}$$

where sv_{ij}^{k+1}, ad_{ij}^{k+1} (i,j = 1:3), sv_f^k, sv_o^k, ad_f^k, ad_o^k and ad_{ij}^k (i,j = 1:3) are the time dependent discretization terms associated with water levels h_i^k, h_i^{k+1} and salinity concentrations c_i^k, c_i^{k+1} ($i = 1{:}3$) at the discretization points of the channel and inflow Q_{in} and outflow Q_{out} discharges. All these terms are a function of the surface (wetted) area of the discretization point (See Appendix A), therefore they are a function of the water levels (h_i^{k+1}) at the next time step $k+1$. Multiplication of these terms with the state vector results in nonlinear constraints for the optimal control problem.

All the other terms in the discretized equations that are not a function of the water level and the salinity concentration at the next time step $k+1$ are placed in the disturbance vector, d_j^k (for example terms that are a function of lateral flows to the channels, which are assumed to be a known disturbance in this study). A more general form of the system dynamics matrix with detailed information of the time dependent discretization terms are provided in Appendix A.

Eq. (4) is defined for a single channel and needs to be extended to a network of channels in order to represent the system dynamics of a polder network. To explain the method, we consider the simple network of three channels with 2 inflows and 1 outflow shown in Fig. 2, where

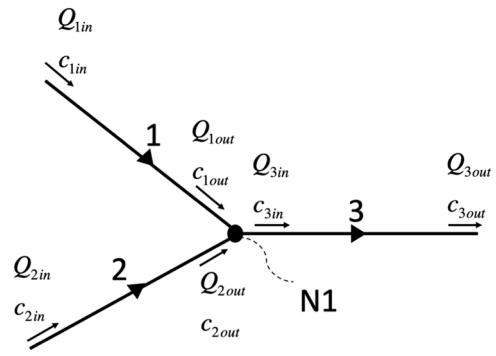

Fig. 2. A simple network of three channels (labeled by 1, 2 and 3) connected at the connection node N1.

the Eqs. (1) and (2) are discretized as in Eq. (4). The full system dynamics of the simple three channel network shown is given as:

$$\underbrace{\begin{bmatrix} E_1 & 0 & 0 \\ 0 & E_2 & 0 \\ 0 & 0 & E_3 \end{bmatrix}^{k+1}}_{\mathbf{E}^{k+1}\in\mathbb{R}^{n_x\times n_x}} \underbrace{\begin{bmatrix} x_1 \\ x_2 \\ x_3 \end{bmatrix}^{k+1}}_{\mathbf{x}^{k+1}\in\mathbb{R}^{n_x}} = \underbrace{\begin{bmatrix} A_1 & 0 & 0 \\ 0 & A_2 & 0 \\ 0 & 0 & A_3 \end{bmatrix}^{k}}_{\mathbf{A}^k\in\mathbb{R}^{n_x\times n_x}} \underbrace{\begin{bmatrix} x_1 \\ x_2 \\ x_3 \end{bmatrix}^{k}}_{\mathbf{x}^k\in\mathbb{R}^{n_x}} +$$

$$\underbrace{\begin{bmatrix} B_{u1} & 0 & 0 \\ 0 & B_{u2} & 0 \\ 0 & 0 & B_{u3} \end{bmatrix}^{k}}_{\mathbf{B}_\mathbf{u}^k\in\mathbb{R}^{n_x\times(n_u)}} \underbrace{\begin{bmatrix} u_1 \\ u_2 \\ u_3 \end{bmatrix}^{k}}_{\mathbf{u}^k\in\mathbb{R}^{(n_u)}} + \underbrace{\begin{bmatrix} d_1 \\ d_2 \\ d_3 \end{bmatrix}^{k}}_{\mathbf{d}^k\in\mathbb{R}^{n_x}} \tag{5}$$

where $\mathbf{x} \in \mathbb{R}^{n_x}$ is the state vector of the channel network and contains the water level and salinity concentrations at all of the discretization points of each channel, $\mathbf{u} \in \mathbb{R}^{n_u}$ is the input vector for the network that has all of the inflow and outflow discharges of the individual channels. The number of states, n_x, is the sum of the number of states for each channel and depends on the discretization spacing chosen and the length of channels. On the other hand, the total number of the inputs, n_u, is two times the total number of channels (which is 6 for the network given in Fig. 2 having one pair of inflow and outflow for each channel).

In addition to the system dynamics given in Eq. (5), mass conservation at connection nodes has to be considered as a constraint to model a network of channels. As an example, for the network in Fig. 2, mass conservation at node N1 assuming complete mixing is given as:

$$Q_{1_{out}}^k + Q_{2_{out}}^k = Q_{3_{in}}^k \tag{6}$$

$$c_{3_{in}}^k = \frac{Q_{1_{out}}^k \times c_{1_{out}}^k + Q_{2_{out}}^k \times c_{2_{out}}^k}{Q_{1_{out}}^k + Q_{2_{out}}^k} \tag{7}$$

where discharge and salinity concentration entering a channel are represented by $Q_{j_{in}}$ and $c_{j_{in}}$ while the ones leaving a channel are represented by $Q_{j_{out}}$ and $c_{j_{out}}$ ($j = 1,2,3$). Together, the system dynamics given in Eq. (5) and the mass conservation constraints given in Eqs. (6)–(7) can be extended to model the dynamics of any polder network for flushing. The size of the resulting state-space model and number of constraints will depend on the number of channels and how they are connected to each other. For the real case study of Lissertocht catchment shown in Fig. 4, mass balance constraints are created from the polder network graph.

3. Problem formulation and objective function for polder flushing

The NMPC controller developed in this study aims to keep the water level and salinity concentrations around their predefined set points, h_{ref}

and c_{ref}, respectively. For any discretization point, i, in channel j, described in Eq. (4), deviations of water level, $e^k_{h_{ji}}$, and salinity concentration, $e^k_{c_{ji}}$, from their set point at time step k are:

$$e^k_{h_{ji}} = h^k_{ji} - h_{ref}, \tag{8}$$

$$e^k_{c_{ji}} = c^k_{ji} - c_{ref}. \tag{9}$$

For water level control, a hard constraint is implemented using the existing maximum, $\overline{h}$, and minimum, $\underline{h}$, allowable water levels of the polder. However, using a hard constraint is not feasible for salinity control. Due to the salinity characteristics of the polder system, at certain times salinity concentrations higher than the set point can be observed, which sometimes may not be possible to flush out depending on the capacity of the system. On the other hand, salinity concentrations below the salinity threshold are fresher than what is required and, thus, they are not a problem in terms of salinity control. To penalize only the positive violations above the salinity threshold, we introduce a soft constraint as explained in Maciejowski et al. (2002) for salinity control and depicted in Fig. 3. Soft constraints on salinity concentration are implemented using a combination of a virtual input, u^* , and a virtual state, $e_c{}^*$.

Virtual state, e^*_c, has a very high penalty in the objective function and is activated only if there is a positive violation of the salinity concentration. Fig. 3 illustrates a trajectory of salinity concentration (solid blue line), an upper threshold for salinity levels (black dashed line), virtual input (red dash-dotted line), and the virtual state (light blue dotted line).

The last objective, minimizing the usage of freshwater and pumping flow, is achieved by penalizing the inputs corresponding to the flows through the intakes and the pumping station of the network in the objective function. For all hydraulic structures in the polder (5 intakes and 1 pumping station), the discharge can vary between zero and maximum discharge capacity of the structure, $\overline{Q^k_i}(i = 1:6)$.

3.1. Objective function

An objective function is used to formulate the goals of the controller subject to the constraints of the system. Control action is calculated by the minimization of the objective function subject to both equality (system model) and inequality (limits of the states and inputs) constraints of the system over the prediction horizon. In this study, objective function is formulated as a quadratic cost function to deal with both positive and negative deviations of the variables from their set points. The controller is designed to regulate the water level and salinity concentrations at the most downstream discretization points of each channel j in the polder network.

For a finite time interval $[t_k, t_f]$ discretized to N_c number of prediction steps where $N_c \times t_c = t_f - t_k$ and t_c is the control time interval, objective function used in this study for the case study area with $m = 14$ channels, $p = 5$ intakes and 1 pumping station is as follows:

$$\begin{aligned}
\min J = & \sum_{j=1}^{m=14}\sum_{i=1}^{N_c}\Big\{e_{h_j}(k+i|k)^T Q_{e_h} e_{h_j}(k+i|k) + \\
& (e^*_{c_j}(k+i|k))^T Q_{e_c}(e^*_{c_j}(k+i|k))\Big\} + \\
& \sum_{j=1}^{p=5}\sum_{i=1}^{N_c}(Q_{j_{in}}(k+i|k))^T R_{Q_{in}}(Q_{j_{in}}(k+i|k)) + \\
& \sum_{i=1}^{N_c}(Q_{pump}(k+i|k))^T R_{Q_{pump}}(Q_{pump}(k+i|k)) + \\
& \sum_{j=1}^{m=14}\sum_{i=1}^{N_c}\Big[u^*_j(k+i|k)^T R_{u^*} u^*_j(k+i|k)
\end{aligned}$$

subject to

the system dynamics given in Eq. (5) extended to 14 channels

mass balance constraints at all connection nodes similar to Eqs. (6)-(7)

$$\begin{aligned}
e^k_{h_j} &= h^k_j - h_{ref} \\
e^k_{c_j} &= c^k_j - c_{ref} \\
e^{*k}_{c_j} &= e^k_{c_j} - u^*_j \\
\underline{h} \le h^k_{ji} &\le \overline{h} \\
0 \le e^{*k}_{c_j} & \\
u^*_j &\le 0 \\
0 \le Q^k_j &\le \overline{Q^k_j}
\end{aligned} \tag{10}$$

where e_{h_j} and e_{c_j} are the deviation of water level and salinity from their set points and $e_{c_j}*$ is the virtual state for salinity control at the most downstream discretization point of channel j, $Q_{j_{in}}$ and Q_{pump} are the manipulated flushing and pumping discharges of the polder, Q_{e_h}, Q_{e_c}, $R_{Q_{in}}$, $R_{Q_{pump}}$ and R_{u^*} are the weights penalizing the corresponding states and input variables (see Table 3 for their values), $\underline{h}$ and $\overline{h}$ are the minimum and maximum allowed water levels and $\overline{Q^k_j}$ is the maximum discharge capacity of the structure j.

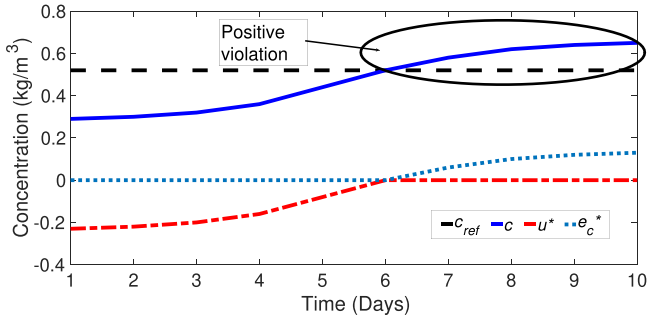

Fig. 3. Illustrative figure for showing the application of the soft constraint for salinity control. Only the positive violations above the salinity threshold, c_{ref}, are penalized in the objective function with the virtual state, e^*_c. Virtual state is equal to zero if the salinity concentration is below or equal to the salinity threshold.

4. Test case description and results

4.1. Lissertocht catchment

To illustrate the closed loop performance of the proposed NMPC scheme based on real-world saline groundwater exfiltration data, we performed simulations for controlling the flushing operation of the Lissertocht catchment. The catchment is located approximately 25 km southwest of the city of Amsterdam (Fig. 4). It can be considered as a representative deep polder in the Netherlands where the main source of salinity is deep saline groundwater exfiltration through boils that are preferential flow paths intersecting the Holocene cover layer (De Louw et al., 2010). The discharge and concentration of the boils are rather constant while the other sources of salt, ditch and drain exfiltration, have temporal variations. Different sources of the saline groundwater exfiltration in the Lissertocht catchment have been studied and modelled in Delsman et al. (2013). Spatial variation of boils in the Lissertocht catchment (see red dots in Fig. 4), results in heterogeneity in salinity disturbance. Salinity concentration variation in the ditches of the Lissertocht catchment is given in between 0.136 and 5.453 kg/m^3 (Delsman et al., 2013). Upstream main channels close to the intakes have fresh water, while the downstream main channels are affected by the boils and higher salinity concentrations are observed. To decrease the surface water salinity, freshwater is supplied through five inlets with

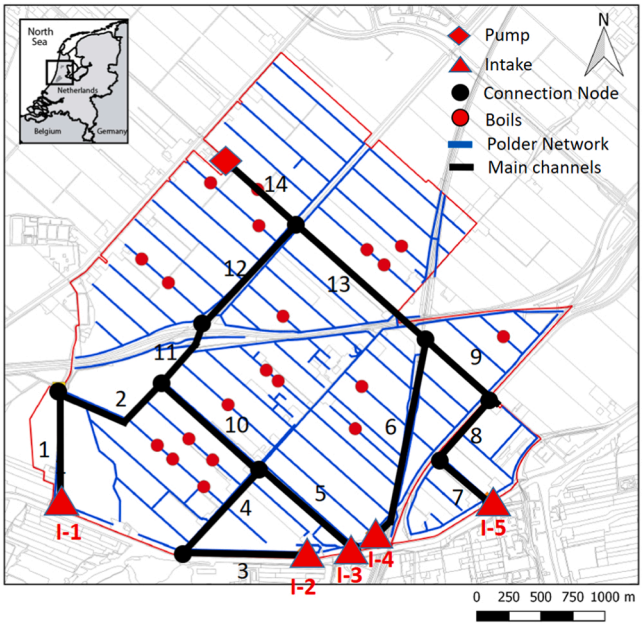

Fig. 4. Location of the Lissertocht catchment (top left) and the layout of the controlled network of the main channels (14 in total with 9 connection nodes), intakes (labeled as I-1 to I-5), pump station and the boils in the area.

a total capacity of 0.0956 m^3/s (see Table 1 for the capacity of each intake). A main pumping station with a capacity of 1.48 m^3/s is used to maintain the water level around the set point, h_{ref}. In this study, we focused on these five intakes and the main pumping station as the control structures used to regulate the water level and salinity concentration in the polder. The main land use in the area is agriculture and the salinity concentration and water quantity requirement of the farmers varies depending on the crop cultivated.

In Aydin et al. (2019a), we optimized the salinity sensor placement for real time control of polder flushing in the main channels using salinity data set of the Lissertocht catchment. The details of the models used and the data set is not the focus of this manuscript and can be found in Aydin et al. (2019a). Similarly, in this study we focused on controlling the salinity concentration and water quantity of the main channels of the Lissertocht catchment (Fig. 4) that transfer the freshwater from intakes to the pumping station. To test the performance of the NMPC scheme, we selected a 30 day dry period (8 May 2013–6 June 2013 shown in Fig. 5) with a very intense rainfall in between Aydin et al. (2019a). We model the Lissertocht catchment with 14 main channels, depicted with numbers in Fig. 4, aggregating a number of connected main ditches. Drainage channels with a connection to the main channels are represented as lateral flows to the main channels transporting the excessive water in the polder parcels collected by the drainage system. Drainage channels can provide a buffer for water level variations and salt load in the polder and during severe drought, flow from main channels to the drainage channels can be observed. However, in accordance with the characteristics of the selected test period in this study, water flows and the associated inflow concentrations from these drainage channels to the main channels are used as known disturbances based on real-world

Table 1
Maximum capacities of the intakes.

Structure	Maximum Capacity [m^3/s]
Intake 1	0.0162
Intake 2	0.0236
Intake 3	0.0306
Intake 4	0.0097
Intake 5	0.0155

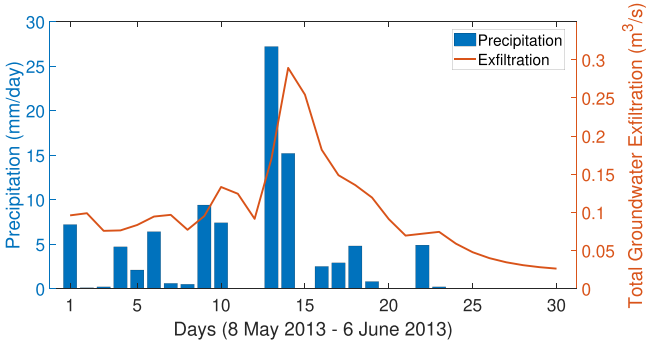

Fig. 5. Selected test period for the NMPC scheme. Daily precipitation (mm/day) is shown on the left and the resulting total groundwater exfiltration (m^3/s) data, as we modeled in Aydin et al. (2019a), used as the disturbance is shown on the right. The forcing data used and parameters of the model in this paper will be available from the corresponding author at request.

saline exfiltration data of the catchment as modelled in Aydin et al. (2019a).Table 2.

4.2. Parameters for modelling and control

In this work, our control goal is to maintain the water level around the set point of − 6.45 m in the polder with a maximum deviation of ± 0.05 m. For salinity level control, a salinity threshold of 1.5 kg/m^3 (= 1500 mg/l) is imposed in accordance with the requirements of the responsible water authority of the area, the Rijnland District Water Control Board. We controlled the water level and salinity concentration at the end of each main channel.

For the spatial discretization of Eq. (10), we used a discretization spacing of 50 m and for the temporal discretization, we used 1 min as the simulation time step and 1 h as the control time interval, t_c. To capture the slow dynamics of the salt transport, we implement a prediction horizon of 24 h resulting in 24 prediction steps, N_c, for the controller. The system model consists of 12528 states (water level and salinity concentration deviations and the virtual states), 1008 control inputs (inflows, outflows and the virtual inputs), 9 connection nodes and 28 water level and salinity concentration control points.

Weight used in Eq. (10) are filled with the values given in Table 3 for each channel of the network depending on the state or input penalized. As an initial guess for the weights penalizing the states and the inputs used in this study, we used the maximum allowed value estimate (MAVE) described in Van Overloop (2006). An estimate of how much a state or a control input may vary is selected as the MAVE of that variable. For example, a MAVE of 0.05 m was used for the water level deviation, which is equal to the allowed deviation from the water level set point

Table 2
Properties of the channels of Lissertocht Catchment.

Channel	Length [m]	Bed width [m]	Side slope [V: H]	Mean Water Depth [m]
1	822	1.40	1	1.12
2	931	2.50	2	0.95
3	915	1.65	1	1.12
4	850	1.40	1	1.12
5	970	1.65	1	0.62
6	1550	1.00	2	1.02
7	450	1.40	2	0.97
8	616	2.00	3	0.97
9	730	2.00	2	0.82
10	1000	1.45	2	1.02
11	550	4.00	2	0.82
12	1070	5.00	2	0.91
13	1330	4.20	2	0.95
14	657	4.20	2	0.95

and the weight in the objective function is calculated as the reciprocal of the square of the MAVE as $1/(0.05)^2 = 400$. Following similar approaches for the other states and inputs penalized, and analyzing results of different settings, we decided on the values given in Table 3 that ensures no violation of the water level constraints.

4.3. Results

The described NMPC framework is used to control the water level and the salinity concentration of the Lissetrocht catchment. The simulation results are presented in Figs. 7–8. To illustrate the difference between the current flushing practice in the Lissertocht catchment (fixed flushing during the crop growing season), the results of the NMPC scheme is compared with fixed flushing. All computations were performed within MATLAB R2019a installed on a 3.50 GHz Intel Xeon machine with 16 GB of ram running Windows 10. The acceptable tolerance of constraint violation option of IPOPT was set to 10^{-3}. We limited the maximum number of iterations to 100, and the average control computation time resulted in 120 s which is much smaller than the control time step of 1 h.

Fig. 6 shows the controlled water level at the downstream end of the catchment close to the pumping station. As can be seen, NMPC keeps the water level around the set point of − 6.45 m. Due to the hard constraint introduced for the water level control and the high penalty for water level deviation (Table 3) in the optimization problem, water levels in all channels stay around the water level set point. The fluctuations in the water level are in the order of millimeters and they are within the predefined upper and lower bounds of water level. The NMPC scheme successfully controls the water level by reacting to the disturbances from groundwater exfiltration shown in Fig. 5.

The controlled discharges of the inlet gates are shown in Fig. 7 for the whole test period (a moving average over 24 h for better visualization). All of the gates have an initial flow of 0.05 m^3/s and the NMPC scheme immediately increases the flows at the beginning of the test period. This behavior is a reaction to the increasing salinity concentrations in the main channels of the polder. As can be seen in Fig. 8(a,c,d,f), the salinity concentration at these channels increases due to the mixing of the boils in those channels. NMPC uses a 24 h prediction horizon and therefore, reacts to these predicted violations of salinity concentrations as soon as possible and increases the intake discharge. Maximum capacities of the intakes, which are used by the fixed flushing strategy over the whole simulation period, are shown with dashed red horizontal lines in Fig. 7 (a)-(e). As can be seen, the NMPC scheme operates the system using flushing discharges close to the individual capacities of the intakes except intake I-4 (Fig. 7(d)) which has the lowest capacity compared to the other intakes. The pumping discharge shown in Fig. 7(f) shows

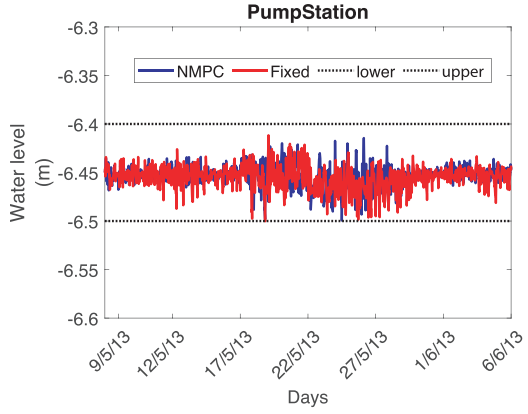

Fig. 6. NMPC controlled water level at the downstream end of Lissertocht catchment compared with fixed flushing, together with upper and lower bound constraints on water level.

Table 3
Weights in the objective function Eq. (10).

Description	Abbreviation	Value [-]
Deviation of water level, e_h	Q_{e_h}	400
Deviation of virtual state, $e_c{}^*$	Q_{e_c}	5
Virtual input, u^*	R_{u^*}	10^{-5}
Flushing discharge, Q_{flush}	$R_{Q_{in}}$	10^{-2}
Pumping discharge, Q_{pump}	$R_{Q_{pump}}$	10^{-2}

similar behaviour for both options, fixed flushing resulting in a slightly higher pumping, as expected. The total volume of water used by each intake and the total volume of flushing and pumping are reported in Table. 4. The total freshwater savings compared to the fixed flushing is 19.5% while the savings in pumping volume is lower at 11.9%, since the system also pumps out later inflows that drain into the channels. The individual savings from each intake varied between 12.0% and 35.5%.

Fig. 8 shows the salinity concentrations at the downstream end for six main channels. These six main channels either have saline boils in them (eg. main channel 14 in Fig. 4) or have a direct connection to drainage channels with saline boils (eg. main channels 2,6,11,12, and 13). Therefore, the salinity concentration in these channels exceeds the salinity concentration threshold set by irrigation requirements. Moreover, depending on the location of the channel in the polder one or more intakes can provide freshwater to these main channels. For example, main channel 2 can only be flushed using the intake I-1, while intakes I-1 to I-3 can provide freshwater for main channel 11 as can be seen in Fig. 4, making this main channel fresh for the most of the considered time. The remaining eight main channels in the catchment (main channels 1–10 except 2 and 6) have no boils connected to them and the ditch exfiltration into these channels is fresh. Therefore, salinity in these channels remains fresher and within constraints.

In terms of salinity control, in this model run, it is clear that the NMPC scheme does not perform as well as the water level control. However, comparison with the fixed flushing gives much more information in terms of the capacity of the system and therefore the performance of the NMPC scheme. The dashed lines in Fig. 8(a)-(f) show the salinity concentrations at the end of each channel with fixed flushing. This is a benchmark for the NMPC scheme, since the NMPC uses values close to the flushing capacity for most intakes. Salinity concentration at these points cannot drop below this level with the given flushing capacity of intakes. For example, as can be seen in Fig. 8(a), the salinity concentration drops below the threshold of 1.5 kg/m^3 only around the date 20/05/13. This corresponds to the period of the simulation when the intensive rainfall results in a peak in (fresh) groundwater exfiltration, which flushes the catchment naturally. The NMPC scheme achieves the salinity level control goal in the main channels 11 and 13 (Fig. 8(c) and (e)). On the other hand, the NMPC scheme fails to drop the salinity concentration below the threshold for the other four main channels presented in Fig. 8. Main channels 12 and 14 are at the downstream end of the network, and they carry most of the high saline water to the pumping station. Therefore, higher salinity concentrations are observed in these two main channels. Moreover, as can be seen in Fig. 8(d)&(f), the performance of the fixed flushing is also not good for main channels 12 and 14 and the salinity concentrations are close to the values achieved by the NMPC. The biggest difference in terms of salinity control performance between fixed flushing and NMPC is observed in main channels 2 and 6 (Fig. 8(a-b)). These two main channels are on the upstream side of the catchment, where main channel 6 can only be flushed by intake I-4 (directly connected to main channel 6) and main channel 2 can only be flushed by intake I-1 (freshwater should first be transported through main channel 1) - see also Fig. 4. The NMPC scheme prefers not to use the full capacity of intakes I-1 and I-4 and saves water in exchange for higher salinity in two main channels. This is a trade-off between salinity and freshwater usage and it is further elaborated in the

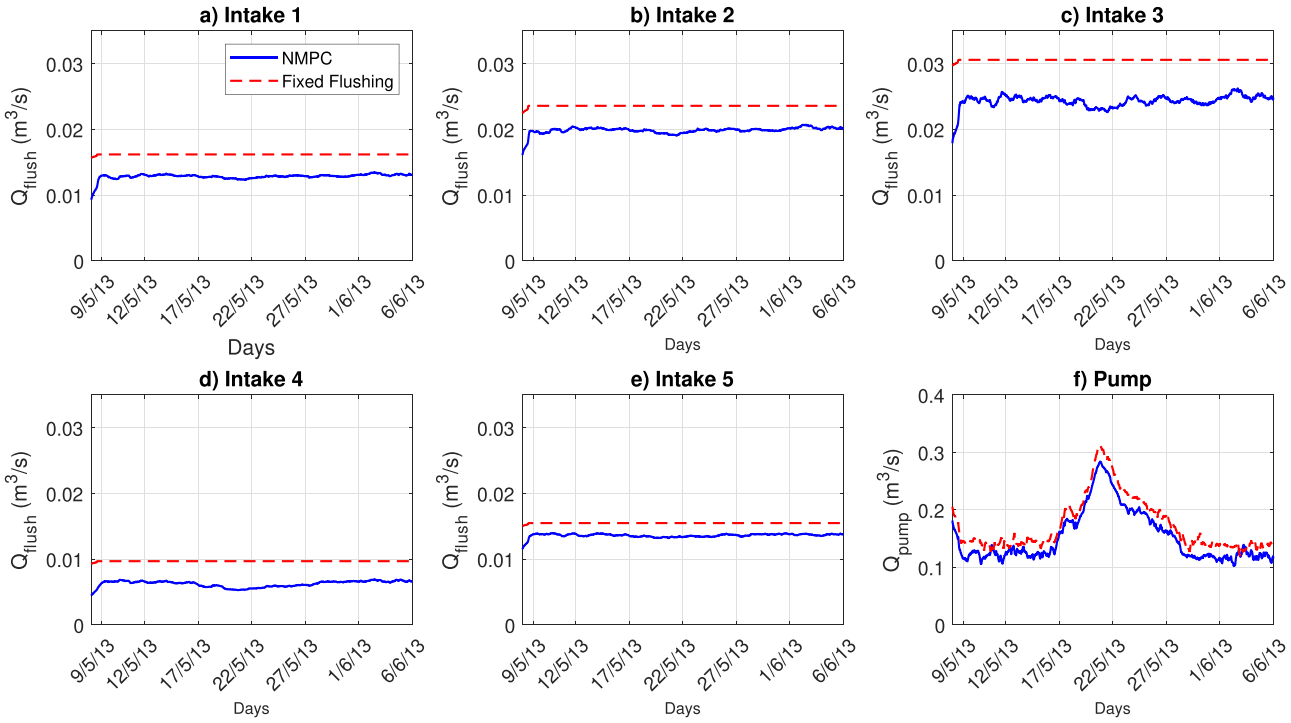

Fig. 7. Controlled discharges (m^3/s) of the intakes (a-e) and the pumping station (f) represented with a moving average of 24 h for smoothing. Discharges used for fixed flushing are represented by the dashed lines which are also the upper limit of the intakes.

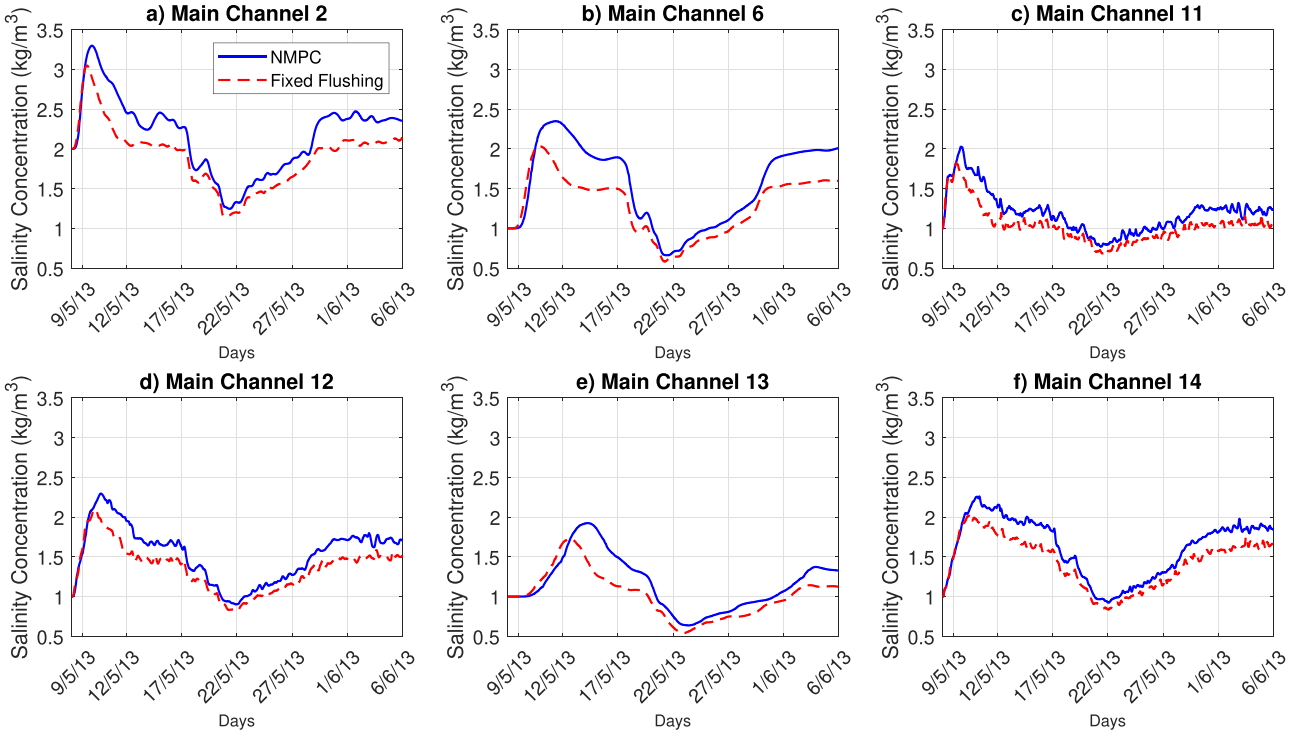

Fig. 8. Controlled salinity concentrations over the simulation period at six different channels of the Lissertocht catchment. a) Main Channel 2, b) Main Channel 6, c) Main Channel 11, d) Main Channel 12, e) Main Channel 13 and f) Main Channel 14. (see Fig. 4 for the locations of the main channels).

next paragraph.

Salinity control performance is directly related to the amount of freshwater usage. Combining the information given in Table 4 and Fig. 8, it can be concluded that there is more freshwater availability for intakes I-1 and I-4 that should be able to dilute the salinity concentration in main channels 2 and 6, respectively. However, as can be seen in Table 4, the capacities of intake I-1 and I-4 are utilized the least compared to the other intakes. At first, the reason why the NMPC does not utilize the maximum capacities of intakes I-1 and I-4 to decrease the higher concentrations in the upstream main channels 2 and 6 was not apparent. A posteriori analysis of the polder network and the results reveal a possible reason related to the flushing capacities and the salt

Table 4
Comparison of NMPC and fixed flushing water usage over the simulation period.

	NMPC [m^3]	Fixed [m^3]	% Saved
Intake 1	3.33×10^4	4.19×10^4	20.6
Intake 2	5.14×10^4	6.11×10^4	15.7
Intake 3	6.30×10^4	7.92×10^4	20.4
Intake 4	1.61×10^4	2.51×10^4	35.5
Intake 5	3.53×10^4	4.01×10^4	12.0
Total	1.99×10^5	2.47×10^5	19.5
Pump	3.94×10^5	4.48×10^5	11.9

transport dynamics described by the AD equations. When a channel is flushed, water with high salinity concentration in the channel is transferred to the downstream channels of the polder and finally pumped out of the system. If a channel is not flushed, salinity concentration in that channel will increase locally and later, through very slow dispersive mechanism, will spread to the rest of the polder. The NMPC makes use of this behaviour defined by the system dynamics in the constraints and decides to transport less salt water from main channels 2 and 6 to the downstream channels. By carrying less salt water downstream, it decreases the need for freshwater usage in the remainder of the polder. Alternative routes that carry fresher water are preferred to flush the downstream channels. For example, downstream of main channel 2 and 6 are main channels 11 and 13, respectively. As shown in Fig. 8, salinity concentrations in these two downstream main channels are most of the time below the salinity threshold. Freshwater necessary to decrease the salinity is mostly provided by alternative routes through intakes I-2, I-3 and I-5. Freshwater provided by these three intakes travels without mixing with saline groundwater through at least one main channel and reaches downstream as a 'fresher' water source. In the considered case here, since the salinity concentrations are controlled in all main channels with equal weighting, the NMPC scheme allows higher concentrations in channels 2 and 6 in exchange for saving freshwater use, which is one of three weighted objectives for the controller.

In the next section, we consider upgrading intake capacity as a future possibility for the stakeholders to guarantee lower salinity levels. Based on simplistic mixing, we propose potential upgrades in intake capacity and test their performance both under fixed flushing and under the advanced NMPC schemes.

4.4. System update to improve the salinity control performance

Results presented in the previous section showed that the salinity control performance was hampered by insufficient capacity of intakes I-1 and I-4. As described in detail in the previous section, main canals 2 and 6 had very large salt loads draining into them but were serviced by intakes I-1 and I-4, respectively, which did not have high enough capacities to dilute them sufficiently. Therefore, in this section, we provide a simple system update by increasing the capacities of these intakes to improve the salinity control performance of the NMPC framework. We focus on decreasing the salinity concentration in main channels 2 and 6 so that the NMPC could choose to flush them to downstream channels when favorable. To allow the NMPC to flush these channels, we calculated the maximum salt loads (summation of the multiplication of all saline groundwater exfiltration discharges with its concentration discharging to these channels). We then used this maximum salt load to calculate the minimum freshwater intake levels from I-1 and I-4, respectively, required to dilute these channels to the salinity threshold of 1.5 kg/m^3 (summation of all the salt load of all fresh and saline flows equal to the threshold). Of course, the capacities could be further increased to trade-off water quality levels with freshwater use. By considering the worst scenario of no rain to naturally flush the system and the number of existing boils discharging (directly or through drainage channels) to these two main channels, we estimated the necessary freshwater intake to dilute the high saline water in these main channels using Eqs. (6)–(7). We increased the capacities of intake I-1 from 0.0162 m^3/s to 0.0342 m^3/s and of intake I-4 from 0.0097 m^3/s to 0.0136 m^3/s, respectively to bring average salinity levels to below the threshold of 1.5 kg/m^3. Keeping the rest of the parameters as the original setting, we simulated the system and the results are presented in Figs. 9-10, where also results of the original configuration and fixed flushing with the updated capacities are included for comparison. Fig. 9 presents the controlled discharges of the intakes and the pumping station. Full capacity of all intakes were used by the fixed flushing and are shown with a dashed line. Similar to Fig. 7, all of the intakes start with an initial flow and the NMPC immediately increases the flushing from all of the intakes. Due to the increased capacities, flushing through intakes I-1 and I-4 is increased as expected for the upgraded case where the NMPC scheme is applied. The rest of the intakes behave similarly to the original setting (i.e. Fig. 7).

The salinity control performance of the updated system (both fixed flushing and NMPC) compared with the original configuration (NMPC) is shown in Fig. 10. Compared to the original configuration (blue lines in Fig. 10), both fixed flushing (red dashed line in Fig. 10) and the NMPC (black dotted line in Fig. 10) of the updated system brings the salinity concentrations in main channels 2 and 6 below salinity threshold (See between the dates 12/5/2013 and 17/5/2013 in Figs. 10(a)-(b)). As expected, due to the increased intake capacities, fixed flushing resulted in the lowest salinity concentrations in all channels. Using the full capacity of the intakes, salinity concentrations in all channels dropped below the salinity threshold (i.e. it is possible to intake the maximum freshwater possible and so reduce peak salt loads in the whole system, albeit using more freshwater than necessary). The NMPC scheme utilized the increased capacities of intakes I-1 and I-4 and additional freshwater from these intakes to dilute and flush the high saline water in the main channels 2 and 6; see Figs. 10(a)-(b). In comparison to the fixed flushing, NMPC did not use the full capacity of the intakes but only the necessary amount (calculated by the optimization) to bring the salinity concentration to the salinity threshold of 1.5 kg/m^3 in the upstream channels. As a result of additional flushing water used, salinity control performance of the NMPC scheme significantly improved in all channels.

For the updated system, the NMPC scheme used around 20% less freshwater compared to the fixed flushing (2.46×10^5 m^3 for the NMPC and 3.05×10^5 m^3 for fixed flushing). For both fixed flushing and NMPC, the better salinity performance comes at the price of using more freshwater from the increased capacities (around 19% increase).

5. Conclusion

In this paper, we propose a novel NMPC framework for optimal flushing control in polders. We presented a network model to optimize multiple objectives and tested the controller in a low-lying Dutch polder, the Lissertocht catchment as a case study. The proposed NMPC scheme is mathematically explained, implemented and used for this case study to control salinity concentration and water quantity in all main channels of the network in simulation experiments. Sufficient performance for water level control was achieved by keeping the water level always within set boundaries. Salinity control performance of the NMPC, however, appeared to be unsatisfactory due to the limited intake capacity. Post analysis of the network and the NMPC results allowed us to determine a simple design update of the system. We achieved a satisfactory salinity control performance by updating the intake capacity of two intake gates. Both in the original and updated system, freshwater usage is reduced by around 20% using the NMPC compared to the fixed flushing strategy presently in operation in the Lissertocht catchment. We believe that the framework presented in this paper is one of the first steps towards the application of NMPC schemes for better management of freshwater resources in irrigation polders. It is useful for irrigation water management in low-lying delta areas with shallow-saline groundwater. Further research on coupling this NMPC scheme with irrigation scheduling optimization frameworks will provide valuable information for the

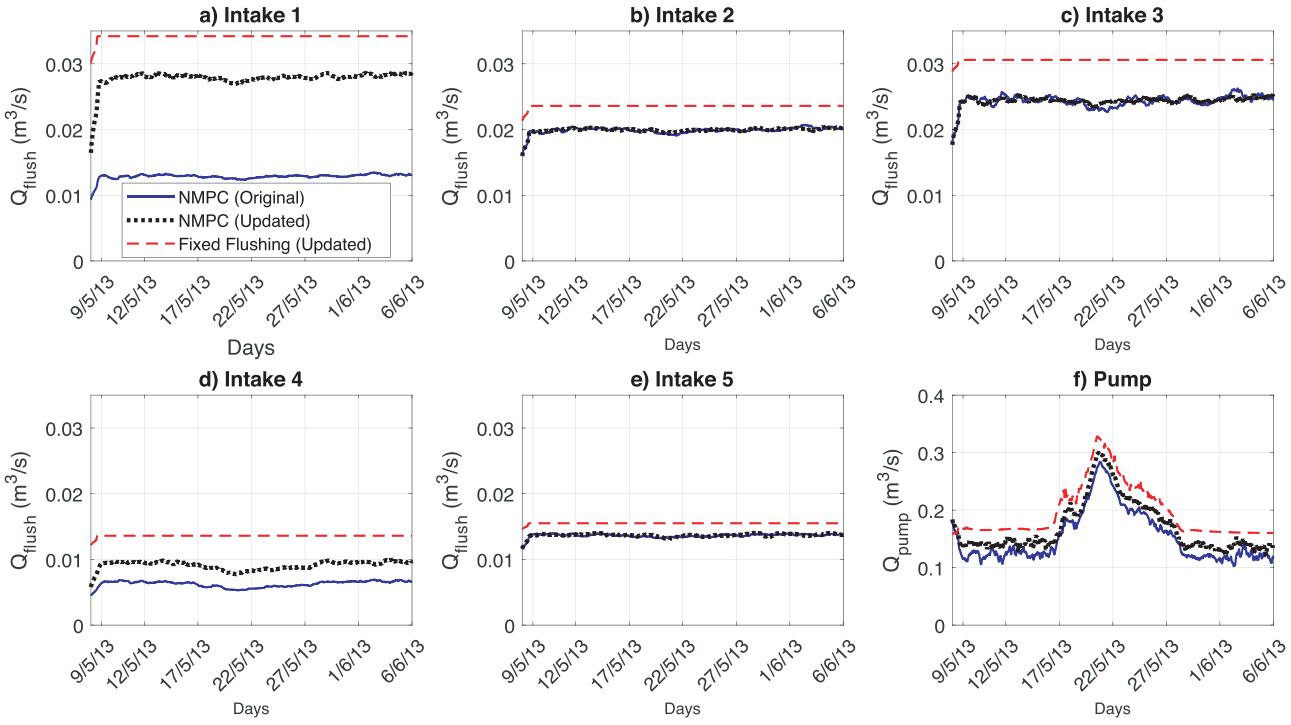

Fig. 9. Controlled discharges (m^3/s) of five intakes (a-e) and the pumping station (f) for the updated system (dotted line) compared with the original configuration (continuous line) and fixed flushing using the updated capacities (dashed line). For smoothing and better representation of the results, all discharges are represented with a moving average of 24 h in this figure. (For interpretation of the references to colour in this figure, the reader is referred to the web version of this article.)

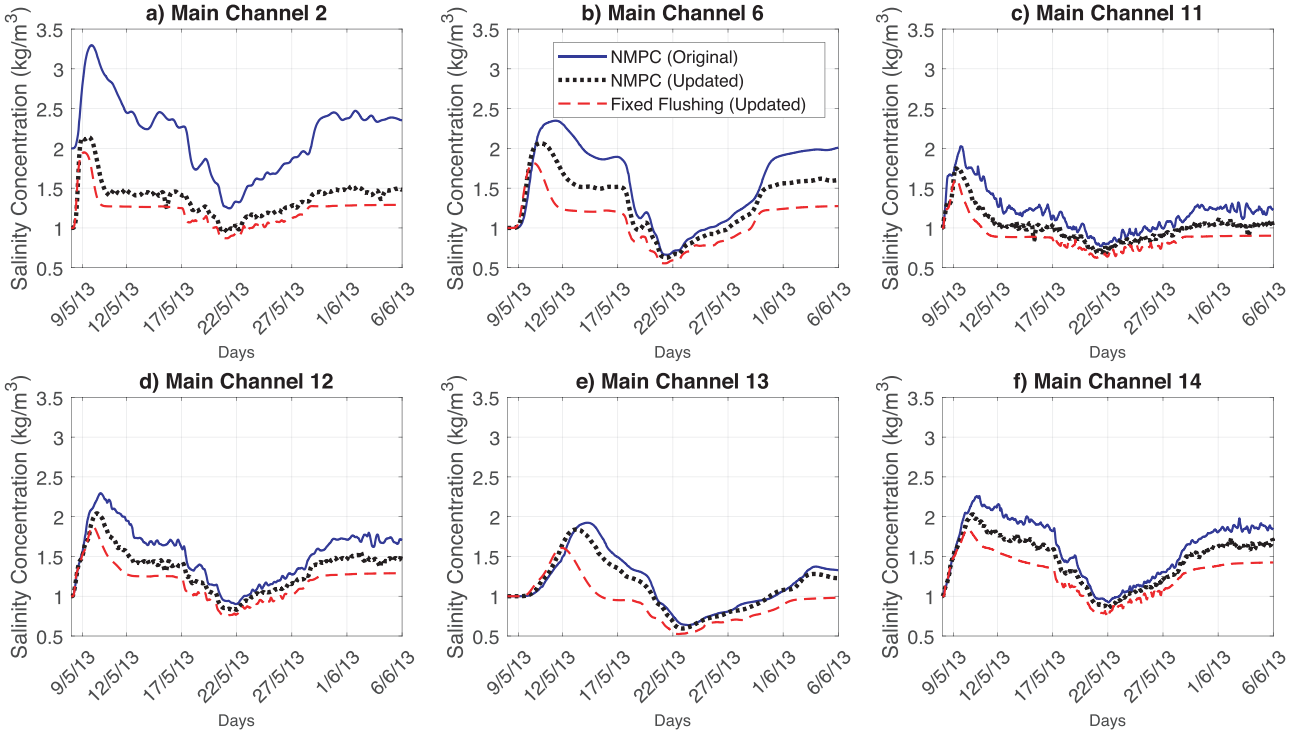

Fig. 10. Controlled salinity concentrations over the simulation period at six different channels of Lissertocht catchment for the updated system compared with the original configuration and fixed flushing using the updated capacities. a) Channel 2, b) Channel 6, c) Channel 11, d) Channel 12, e) Channel 13 and f) Channel 14. Channel numbers are shown in Fig. 4.

sustainable management of irrigation agriculture.

Declaration of Competing Interest

The authors declare that they have no known competing financial interests or personal relationships that could have appeared to influence the work reported in this paper.

Acknowledgements

This research is financed by the Netherlands Organization for Scientific Research (NWO), which is partly funded by the Ministry of Economic Affairs and Climate Policy, and co-financed by the Netherlands Ministry of Infrastructure and Water Management and partners of the Dutch Water Nexus consortium.

Appendix A

Saint Venant and Advection Dispersion equations are discretized using a staggered grid scheme. A system dynamics matrix discretization matrix (see equation (4)) for n discretization points is obtained with the terms given as:

$$For\ i=1$$

$$sv_{i,i}=1+\frac{\Delta t}{A_{s,i}^{n}}A_i^k fu_{i+1/2},\ \ sv_{i,i+1}=-\frac{\Delta t}{A_{s,i}^{k}}A_i^k fu_{i+1/2},\ \ sv_f=-\frac{\Delta t}{A_{s,i}^{n}},$$

$$d_i=-\frac{\Delta t}{A_{s,i}^{k}}A_i^k ru_{i+1/2}+\frac{\Delta t Q_{l,i}^k}{A_{s,i}^{k}},$$

$$ad_{i,i}=1+\frac{\Delta t}{V_i^k}\left(\frac{1}{\Delta x}\left(K_{i+1/2}^{k+1}A_{i+1/2}^{k+1}+K_{in}^{k+1}A_i^{k+1}\right)+Q_{i+1/2}^{k+1}\right),$$

$$ad_{i,i+1}=-\frac{\Delta t}{V_i^n\cdot\Delta x}K_{i+1/2}^{k+1}A_{i+1/2}^{k+1},ad_f=\frac{\Delta t}{V_i^k}\left(c_i^k-c_{in}^{k+1}\right),\ \ ad_{i,i}^k=1+\frac{\Delta t\left(Q_{i+1/2}^{k+1}\right)}{V_i^k},d_{i+n}=\frac{\Delta t}{V_i^n}\left(\frac{1}{\Delta x}K_{in}^{k+1}A_i^{k+1}\right)\left(c_{in}^{k+1}-c_{\mathrm{ref}}\right)+\frac{Q_{l,i}^k\Delta t\left(c_{l,i}^n-c_i^n\right)}{V_i^n}$$

For interior discretization points: i=2:n-1

$$sv_{i,i}=1+\frac{\Delta t}{A_{s,i}^{k}}A_{i-1}^k fu_{i-1/2}+\frac{\Delta t}{A_{s,i}^{k}}A_i^k fu_{i+1/2},\ \ sv_{i,i-1}=-\frac{\Delta t}{A_{s,i}^{k}}A_{i-1}^k fu_{i-1/2},$$

$$sv_{i,i+1}=-\frac{\Delta t}{A_{s,i}^{k}}A_i^k fu_{i+1/2},$$

$$d_i=\frac{\Delta t}{A_{s,i}^{k}}A_{i-1}^k\left(ru_{i-1/2}\right)-\frac{\Delta t}{A_{s,i}^{k}}A_i^k\left(ru_{i+1/2}\right)+\frac{\Delta t Q_{l,i}^k}{A_{s,i}^{k}},$$

$$ad_{i,i}=1+\frac{\Delta t}{V_i^k}\left(\frac{1}{\Delta x}\left(K_{i+1/2}^{k+1}A_{i+1/2}^{k+1}+K_{i-1/2}^{k+1}A_{i-1/2}^{k+1}\right)+Q_{i+1/2}^{k+1}\right),ad_{i,i-1}=-\frac{\Delta t}{V_i^k}\left(\frac{1}{\Delta x}K_{i+1/2}^{k+1}A_{i-1/2}^{k+1}+Q_{i-1/2}^{k+1}\right)ad_{i,i+1}=-\frac{\Delta t}{V_i^k}\frac{1}{\Delta x}K_{i+1/2}^{k+1}A_{i+1/2}^{k+1},ad_{i,i}^k$$

$$=1+\frac{\Delta t\left(\left(Q_{i+1/2}^{k+1}\right)-\left(Q_{i-1/2}^{k+1}\right)\right)}{V_i^k},d_{i+n}=\frac{Q_{l,i}^k\Delta t\left(C_{l,i}^k-C_i^k\right)}{V_i^k}$$

For i=n

$$sv_{i,i}^k=1+\frac{\Delta t}{A_{s,i}^{k}}A_{i-1}^k fu_{i-1/2},sv_{i,i-1}=-\frac{\Delta t}{A_{s,i}^{k}}A_{i-1}^k fu_{i-1/2},sv_o=\frac{\Delta t}{A_{s,i}^{k}},$$

$$d_i=\frac{\Delta t}{A_{s,i}^{k}}\theta A_{i-1}^k\left(ru_{i-1/2}\right)+\frac{\Delta t Q_{l,i}^k}{A_{s,i}^{k}},ad_{i,i}=1+\frac{\Delta t}{V_i^k}\left(\frac{1}{\Delta x}\left(K_{i-1/2}^{k+1}A_{i-1/2}^{k+1}\right)\right),$$

$$ad_{i,i-1}=-\frac{\Delta t}{V_i^k}\left(\frac{1}{\Delta x}K_{i-1/2}^{k+1}A_{i-1/2}^{k+1}+Q_{i-1/2}^{k+1}\right),$$

$$ad_o=\frac{\Delta t}{V_i^k}\left(C_i^{k+1}-C_i^k\right)ad_{i,i}^k=1-\frac{C_i^k\Delta t\left(Q_{i-1/2}^{k+1}\right)}{V_i^n},d_{i+n}=\frac{Q_{l,i}^k\Delta t\left(C_{l,i}^k-C_i^k\right)}{V_i^n}$$

Where

$$fu_{i+1/2}^k=\frac{g\Delta t}{\Delta x\left(1+g\frac{v_{i+1/2}^k}{Cz^2R}\right)}$$

$$ru_{i+1/2}^k=\frac{\frac{1}{A_{i+1/2}^k}\left(\frac{\overline{Q}_{i+1}^k v_{i+1/2}^k-\overline{Q}_i^k v_{i-1/2}^k}{\Delta x}+v_{i+1/2}^k\frac{\overline{Q}_{i+1}^k-\overline{Q}_i^k}{\Delta x}\right)+v_{i+1/2}^k}{\left(1+g\frac{v_{i+1/2}^k}{Cz^2R}\right)}$$

$$\overline{Q}_i^k=\left(Q_{i+1/2}^k-Q_{i+1/2}^k\right)/2$$

$$\overline{A}_{i+1/2}^k=\left(A_{i+1/2}^k-A_{i+1/2}^k\right)/2$$

K_{in} and C_{in} are the dispersion coefficient and the concentration of the inflow.

References

Alfonso, L., Lobbrecht, A., Price, R., 2010. Optimization of water level monitoring network in polder systems using information theory. Water Resour. Res. 46.

Aydin, B.E., van Overloop, P.J., Rutten, M., Tian, X., 2016. Offset-free model predictive control of an open water channel based on moving horizon estimation. J. Irrig. Drain. Eng. 143, B4016005.

Aydin, B.E., Hagedooren, H., Rutten, M.M., Delsman, J.R., Oude Essink, G.H.P., van de Giesen, N., Abraham, E., 2019a. A greedy algorithm for optimal sensor placement to estimate salinity in polder networks. Water 11, 1101.

Aydin, B.E., Tian, X., Delsman, J.R., Oude Essink, G.H.P., Rutten, M., Abraham, E., 2019b. Optimal salinity and water level control of water courses using model predictive control. Environ. Model. Softw. 112, 36–45.

Betts, J.T., 2010. Practical Methods for Optimal Control and Estimation Using Nonlinear Programming. Siam, p. 19.

De Louw, P.G., Oude Essink, G.H.P., Stuyfzand, P.J., Van der Zee, S., 2010. Upward groundwater flow in boils as the dominant mechanism of salinization in deep polders, the netherlands. J. Hydrol. 394, 494–506.

De Louw, P.G.B., Eeman, S., Siemon, B., Voortman, B.R., Gunnink, J., Van Baaren, E.S., Oude Essink, G.H.P., 2011. Shallow rainwater lenses in deltaic areas with saline seepage. Hydrol. Earth Syst. Sci. 15, 3659–3678.

Delgoda, D., Malano, H., Saleem, S.K., Halgamuge, M.N., 2016. Irrigation control based on model predictive control (mpc): formulation of theory and validation using weather forecast data and aquacrop model. Environ. Model. Softw. 78, 40–53.

Delsman, J.R., 2015. Saline Groundwater-surface Water Interaction in Coastal Lowlands. IOS Press, Inc, Amsterdam. https://doi.org/10.3233/978-1-61499-518-0-i.

Delsman, J.R., Oude Essink, G.H.P., Beven, K.J., Stuyfzand, P.J., 2013. Uncertainty estimation of end-member mixing using generalized likelihood uncertainty estimation (glue), applied in a lowland catchment. Water Resour. Res. 49, 4792–4806.

Delta Programme Commissioner, 2019. Delta Programme 2020 - Continuing the work on the delta: down to earth, alert, and prepared. Technical Report Delta Programme Commissioner.

Fischer, H.B., List, J.E., Koh, C.R., Imberger, J., Brooks, N.H., 2013. Mixing in Inland and Coastal Waters. Elsevier,.

Hassani, Y., Shahdany, S.M.H., Maestre, J., Zahraie, B., Ghorbani, M., Henneberry, S.R., Kulshreshtha, S.N., 2019. An economic-operational framework for optimum agricultural water distribution in irrigation districts without water marketing. Agric. Water Manag. 221, 348–361.

Hof, A., Schuurmans, W., 2000. Water quality control in open channels. Water Sci. Technol. 42, 153–159.

Kayacan, E., Kayacan, E., Ramon, H., Saeys, W., 2014. Learning in centralized nonlinear model predictive control: application to an autonomous tractor-trailer system. IEEE Trans. Control Syst. Technol. 23, 197–205.

Klijn, F., van Velzen, E., terMaat, J., Hunink, J., Baarse, G., Beumer, V., Boderie, P., Buma, J., Delsman, J.R., Hoogewoud, J. et al. , 2012. Zoetwatervoorziening in Nederland: aangescherpte landelijke knelpuntenanalyse 21e eeuw. Technical Report Deltares.

de Louw, P.G., Velde, Y., Zee, S. v. d., 2011. Quantifying water and salt fluxes in a lowland polder catchment dominated by boil seepage: a probabilistic end-member mixing approach. Hydrol. Earth Syst. Sci. 15, 2101–2117.

Maciejowski, J.M., 2002. Predictive Control: With Constraints. Pearson Education.

Nederkoorn, E., Schuurmans, J., Grispen, J., Schuurmans, W., 2012. Continuous nonlinear model predictive control of a hybrid water system. J. Hydroinform. 15, 246–257.

Oude Essink, G.H.P., Van Baaren, E.S., De Louw, P.G., 2010. Effects of climate change on coastal groundwater systems: a modeling study in the netherlands. Water Resour. Res. 46.

Raats, P.A., 2015. Salinity management in the coastal region of the netherlands: a historical perspective. Agric. Water Manag. 157, 12–30.

Romero, R., Muriel, J., García, I., de la Peña, D.M., 2012. Research on automatic irrigation control: state of the art and recent results. Agric. Water Manag. 114, 59–66.

Sampathirao, A.K., Sopasakis, P., Bemporad, A., Patrinos, P.P., 2017. Gpu-accelerated stochastic predictive control of drinking water networks. IEEE Trans. Control Syst. Technol. 26, 551–562.

Schoubroeck, F. v., Kool, H. 2010. The remarkable history of polder systems in the netherlands.International Consultation on Agricultural Heritage Systems of the 21st Century.

Shang, C., Chen, W.-H., Stroock, A.D., You, F., 2019. Robust model predictive control of irrigation systems with active uncertainty learning and data analytics. IEEE Trans. Control Syst. Technol.

Tavernini, D., Metzler, M., Gruber, P., Sorniotti, A., 2018. Explicit nonlinear model predictive control for electric vehicle traction control. IEEE Trans. Control Syst. Technol. 27, 1438–1451.

Tian, X., van Overloop, P.J., Negenborn, R.R., van de Giesen, N., 2015. Operational flood control of a low-lying delta system using large time step model predictive control. Adv. Water Resour. 75, 1–13.

Van Overloop, P.J., 2006. Model Predictive Control on Open Water Systems. IOS Press.

Wächter, A., Biegler, L.T., 2006. On the implementation of an interior-point filter line-search algorithm for large-scale nonlinear programming. Math. Program. 106, 25–57.

Wang, Y., Puig, V., Cembrano, G., 2017. Non-linear economic model predictive control of water distribution networks. J. Process Control 56, 23–34.

Xu, M., Van Overloop, P.J., Van De Giesen, N., Stelling, G., 2010. Real-time control of combined surface water quantity and quality: polder flushing. Water Sci. Technol. 61, 869–878.

Xu, M., van Overloop, P.J., Van de Giesen, N., 2013. Model reduction in model predictive control of combined water quantity and quality in open channels. Environ. Model. Softw. 42, 72–87.